COMPARISON OF PERFORMANCE OF PROPELLER BLADES BY DIFFERENCE IN PLANAR SHAPE

Nobuyuki ARAI*, Katsumi HIRAOKA*
***Tokai University**
n.arai@tokai-u.jp;hiraoka@keyaki.cc.u-tokai.ac.jp

Keywords: *Wind Tunnel Testing, Propeller, Low Reynolds Number Flow*

Abstract

A blade that has the optimum shape for low Reynolds number field and the other blades that have the characteristic shape, which is trapezoid, were performed to wind tunnel test. Then, the distributions on the surface of these blades were obtained. In order to compare their performances among these blades from a point of view of difference in planar shape of blade, the blade surface was divided up 3 region as "inner", "middle", and "outer", and partial thrust, torque, and efficiency were estimated on the basis of the pressure distribution.

1 Introduction

The propeller is the most efficiency device for propulsion in low speed region and using for the various airplanes which are classified in the normal, commuter, acrobatic, and so on. In the long history, many blades have been developed to adapt to various flight conditions of these kinds of airplane.

Recent years, smaller airplane has been received attention. These have the purpose to fly in the lower Reynolds number region,

In order to determine the planar shape and twist angle of blade which operates in low Reynolds number field, the optimum design method by Adkins & Liebeck[1] have been used. This method is based on the vortex theory, then, if the characteristic of airfoil of cross section is specified, the optimum planer shape can be obtained under the condition of minimum energy loss, which is the approximation that the wake is a constant helix flow proposed by Betz[2]. The optimum shape blade has the strong point that the efficiency of propeller is high. But, if the characteristic of the other blades, which have rectangle, trapezoid, and so on for example, are obtained, the shape of the blade that operates under the specified condition can be improved on the basis of the characteristic.

In this study, in order to compare the thrust, torque and efficiency among the different planar shape blades, three types of blade are experimented in wind tunnel and calculated by CFD. And, the characteristic of these blades were compared from the view point of the different in their planar shapes.

2 Experiment devices

2.1 Propeller blades

In order to obtain the characteristic by the difference in the planar shape, 3 types of blade, Prop00, Prop01, and Prop02, were used. These blades were designed and made for this experiment, and have its own characteristic planar shape.

The common conditions for the design of the blade, which were used for our experiment, are as follow.

- A wing section that remains the high lift in the wide range of the angle of attack is adopted.
- The diameter of propeller is confined to 0.84m because the wind tunnel owned by Tokai University has 1.0 *m* by 1.5 *m* test section area.
- In order to obtain the characteristic of propeller in low Reynolds number, Reynolds number at 80 % position in span direction is 10^5 order.

Table 1 design parameter of propeller blade.

Uniform Velocity	13 *m/s*
Rotation Speed of Propeller	550RPM
Number of blades	2
Wing Section	FX63-137
Radius of Blade	0.42*m*
Position at the Root of Blade	0.06*m*
Maximum of Chord Length	0.177*m*
Minimum of Chord Length	0.061*m*

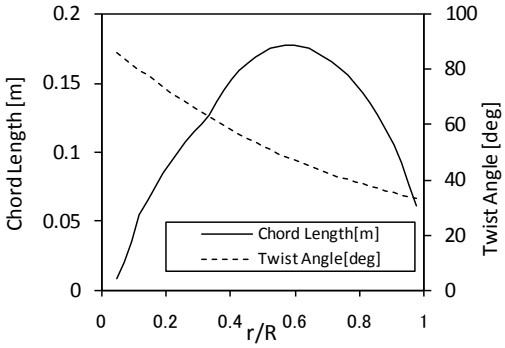

Fig. 1 Twisted Angle and Chord Length of Prop00.

Parameters which are needed for the design are as shown in Table 1.

For the shape of wing section FX63-137 was chosen because it has fine lift-drag ratio in the region that Reynolds number is 10^5, and this property was endured by an wind tunnel test.

The shape of Prop00 blade was designed by the optimum shape design method by Adkins&Liebeck under the conditions as shown in Table 1. The obtained distributions of twist angle and chord length are shown in Fig. 1 and the external appearance of Prop00 blade is as shown in Fig. 2 a).

In order to compare the characteristic of efficiency, pressure distribution, thrust, and torque, the other 2 types of blade, which have different planar shapes, also were used. The blades, Prop01, and Prop02, are as shown in Fig. 2 b) and c). Prop01 blade and Prop02 blade have trapezoid growing larger linearly toward the tip of blade and inverse trapezoid tapering off linearly toward the tip of blade as the plane shape, respectively. All these blades have same solidity and twist angle for the agreement of basic characteristic of shape.

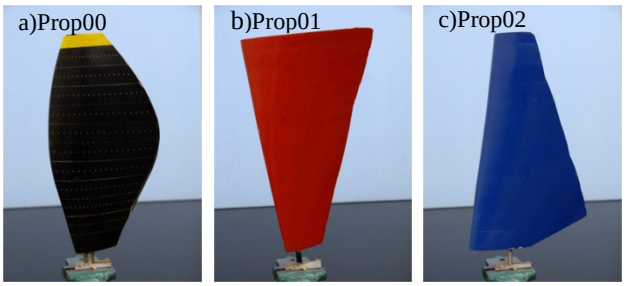

Fig. 2 3 Types of Propeller Blade.

These blades were made of balsa wood. And these were coated with a resin and polished over the whole surface in order to hold down the roughness of the surface.

2.2 Wind tunnel

This experiment was performed by use of a low-speed wind tunnel testing device owned by Tokai University. Maximum wind speed is 40 *m/s*. There is a 6-forces balance device in the test section, which can be employed for thrust measurement of propeller. And as mentioned above, a size of nozzle is 1.0 *m* by 1.5 *m*, then, the span length of our propeller blade results from that.

2.3 Driving devices

As shown in Fig. 3, a driving part, which revolves propeller, consists of a motor, slip ring device, and torquemeter. Each axis is connected on the rotational axis of propeller. The driving part was set on the main strut of 6-forces balance, and all experiments were performed under the environment that propeller rotates in the test section of wind tunnel as shown in Fig. 4.

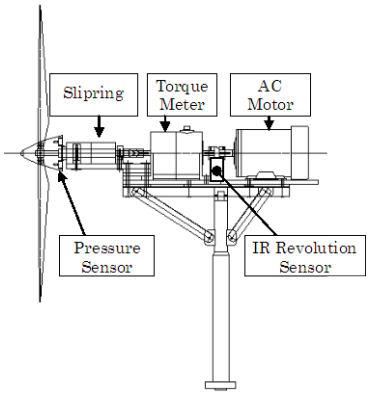

Fig. 3 Devices for Driving and Measuring.

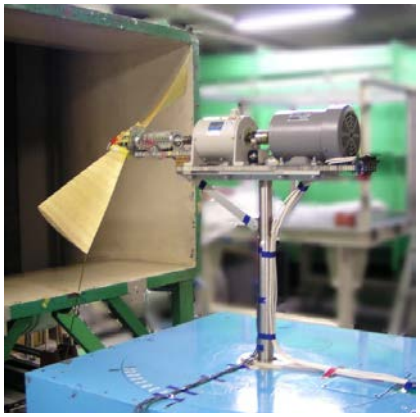

Fig. 4 Scene of Testing in Wind Tunnel.

The rotation of propeller was controlled by exclusive inverter, and the rotation speed was verified by the universal counter which indicates the rotation frequency based on an electrical cyclic signal from the photodiode which receives the infrared reflected by the white-black pattern on the axis.

2.4 Pressure measurement

2.4.1 Method of pressure on surface of the revolving blade

In order to measure the static pressure distribution on the surface of blade, the pressure obtained from a hole that is passed through the opposite side of blade was led to the pressure sensor by a tube. The small holes that its diameter is 1mm were arrayed on the surface as shown in Fig. 5. The number of holes is 319, which is 29 rows in the span direction and 11 columns in the chord direction, on one side.

The holes were limited to be arrayed from 5% to 80% position on the chord line because the leading edge and trailing edge of blade don't have enough thickness to remain its structure if holes are set there. This restriction prevents the estimation of the force based on the pressure distribution on the whole area of blade. But, as mentioned below, by referred an tendency of the pressure distribution by CFD simulation, the thrust and torque can be estimated by the pressure distribution directly measured.

In this experiment, 4 pressure sensors were set in the nose cone, then, the pressure on

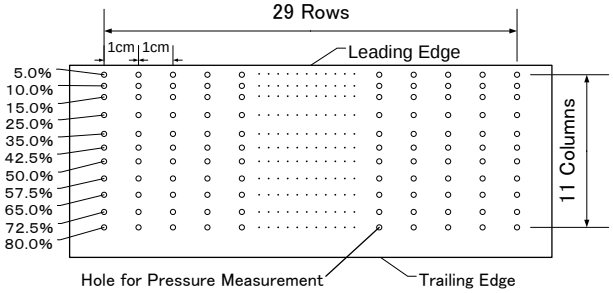

Fig. 5 Holes on a Blade for Pressure Measurement.

the blade rotating was directly obtained. Since there are 4 pressure sensors in the nose cone, the number of holes that are able to measure at once is only 4 points. In measuring the pressure, the pressure on the surface of blade circulates to the pressure sensor in the nose cone by connecting between one hole on the blade, which an aluminum tube is inserted, and one sensor with silicone tube. These aluminum tubes are needed to replace to other holes by hands every 4 holes. Furthermore, the other holes excepting for the 4 holes that are used for measurement were filled in with the solid columnar fragments in order to avoid to leak into the opposite side.

2.4.2 Pressure sensor

The measurable pressure range of this sensor is ±0.25 *kPa*. The data of pressure which is converted by sensor on the blade is recorded by PC through slip ring and A/D conversion. The data of pressure was recorded for 2.5 sec by 10 kHz sampling frequency.

The recorded voltage data was averaged at each measurement point and converted into the pressure value by a calibration data. And obtained gauge pressure was carried out the following correction for centrifugal force.

2.4.3 Correction for centrifugal force

The static pressure on the blade reaches at the pressure sensor by passing through the silicon tube. In this process, the pressure sensor in the nosecone senses the suction pressure due to the centrifugal force because the force acts on the air to the outside in the silicon tube embedded in the rotating blade. Then, in order to remove the extra suction pressure from the measured pressure, a correction formula was considered as blow.

In the tube that keeps rotating with angular velocity ω *rad/s*, the true pressure P_e *Pa* acts at the outer end of tube where is r_e *m* position from the center, and the pressure P_c *Pa* at the center of rotation, which centrifugal force doesn't influence. Supposing that the pressure P_m *Pa* was measured by the sensor that is at r_m *m* position from the center, the true pressure P_e *Pa* is

$$P_e = P_m \cdot e^{\frac{\omega^2}{2RT}(r_e{}^2 - r_m{}^2)} + P_c \cdot e^{\frac{\omega^2}{2RT} r_e{}^2}, \qquad (1)$$

where temperature and gas constant for air are T *K* and R m^2/s^2K.

2.5 Result of pressure distribution

The distributions of pressure coefficient are as shown in Fig. 6. The colored area of that picture, which represents color contour of coefficient value, is limited because there are unmeasurable areas where are the leading edge side beyond 5% position, trailing edge side beyond 80% position on the chord, and near the tip and root side of blade.

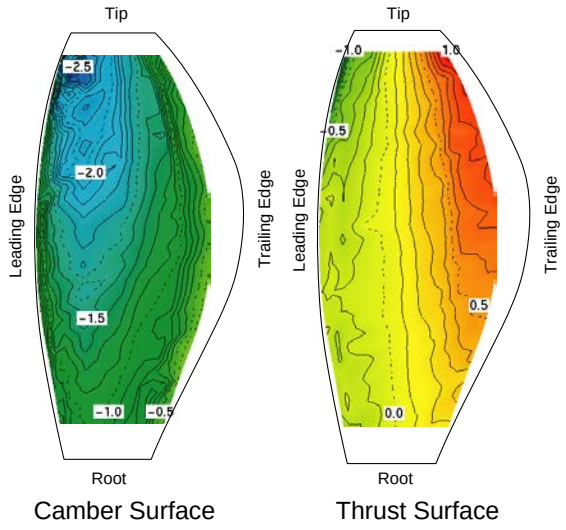

a) Prop00

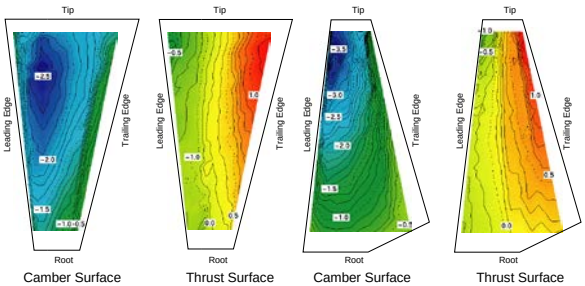

b) Prop01 c) Prop02

Fig. 6 Distribution of Pressure Coefficient by direct pressure measurement.

As shown by the distribution of Prop00 in Fig. 6 a), on the thrust side, there is the tendency that the suction pressure becomes larger as the span position is more outside. And, the space of contour lines changes locally beside the trailing edge, especially at the tip side. This variation of pressure coefficient indicates the characteristic of a short bubble in low Reynolds number region, which the separation and reattachment of the flow occur in a relatively wide extent behind the suction peak[3].

The minimum value of pressure coefficient on the thrust side is -2.73. On the other hand, on the thrust side, the pressure tends to vary equally among chord line toward the tip of blade.

Figs. 6 b) and c) show the distributions of pressure coefficient on Prop01 and Prop02 blades. The minimum pressure coefficient on the thrust side of Prop02 and Prop03 were -2.52 and -3.48 under the standard state, respectively. Also on these two blades, the area that the space of contour lines becomes closely appeared near the trailing edge. This area lies along the trailing edge on Prop01 blade, and near the tip on Prop02 blade.

3 CFD simulation

3.1 Condition of calculation

In order to confirm the result of direct pressure measurement, CFD simulation was performed by usage of FLUENT. 3 types of grid data based on the geometry of actual blades were generated by usage of GAMBIT and TGrid. The conditions for calculation are shown in Table 2. Flow type was chosen as Laminar because the local Reynolds number at each span position is less than 250,000.

An Inlet velocity and an angular velocity of rotation of propeller were set 13*m/s* and 57.6*rad/s*, respectively.

Table 2 Conditions for CFD calculation.

Solver	Pressure based
Scheme	SIMPLEC
Discretization method	2nd order upwind
Flow type	Incompressible ideal flow
	Laminar flow
Mesh	Moving mesh

3.2 Result of CFD simulation

Fig. 7 shows the results of CFD simulation. The values in these figures are pressure coefficient represented by contour lines.

The distribution of pressure coefficient of Prop00 is shown in Fig. 7 a). On the thrust surface, the tendencies that are the position of low pressure region near the tip and the existence of the concentration of contour line, which represents the laminar separation, appear near the trailing edge. These characteristic are

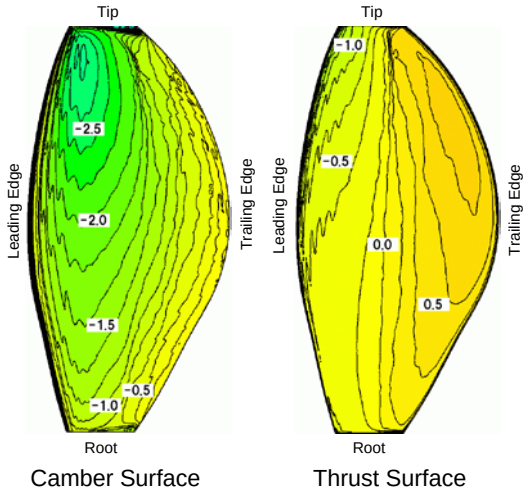

a) Prop00

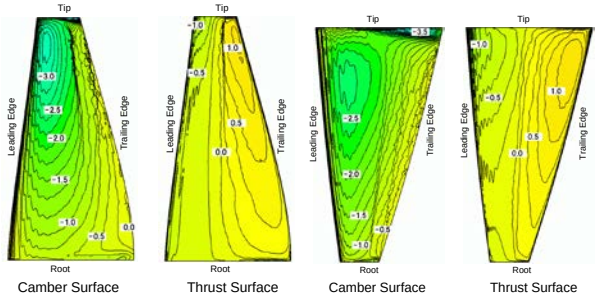

b) Prop01 c) Prop02

Fig. 7 Distribution of Pressure Coefficient by CFD simulation.

similar to the result of direct pressure measurement. In addition to this, distribution of pressure coefficient of the calculation almost agreed with the one of the measurement.

Moreover, as shown in Figs. 7 b) and c), the distributions of other blades, Prop01 and Prop02, have the same tendencies as the direct measurement represents, which are the phenomenon and the value of coefficient.

Therefore, the suitability of the result could be ensured owing to the agreement of each result.

4 Comparison of the evaluation of efficiency

4.1 Interpolation for the result of measurement

As mentioned above, the region of pressure distribution on the surface of blade obtained by the direct measurement is limited because of the thickness of blade. If this limited distribution was referred to evaluate the thrust, torque, and efficiency, a correct value can't be obtained. Then, some sort of method is needed in order to interpolate the pressure distribution in the unmeasurable area on the surface of each blade.

The distribution on whole area of the blade was calculated by CFD simulation and tendency of pressure distribution obtained by both methods matched, but the pressure coefficient didn't strictly agree with the measured value. Then, on the trailing edge side, by referring the tendency obtained by CFD that the pressure increase monotonously toward trailing edge, the value on the unmeasurable area could be estimated by the linear interpolation. By contrast, on the leading edge side, by the assuming the static pressure at the stagnation point, the value could be interpolated because the only linear interpolation of the obtained value can't estimate owing to the rapid variation of the pressure at the leading edge.

Figs. 8, 9, and 10 show the efficiency when the interpolation is applied to the value on the unmeasurable area. The line of "exp. with L_dynamical T_linear" represents the result that the method of the interpolation mentioned above was applied. In comparison with the

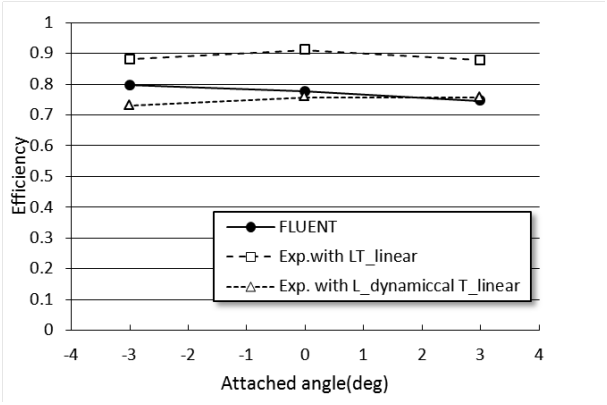

Fig. 8 Efficiency of Prop00 for 3 attached angles.

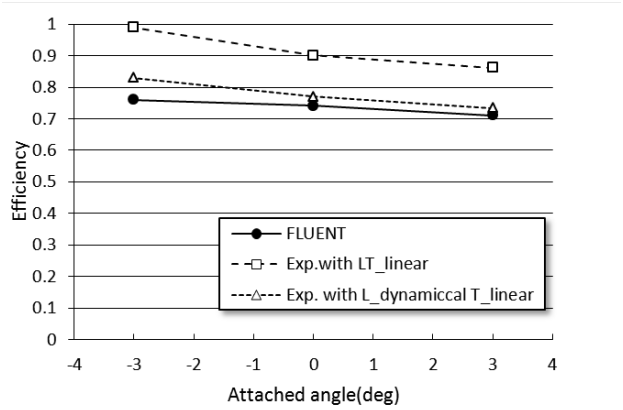

Fig. 9 Efficiency of Prop01 for 3 attached angles.

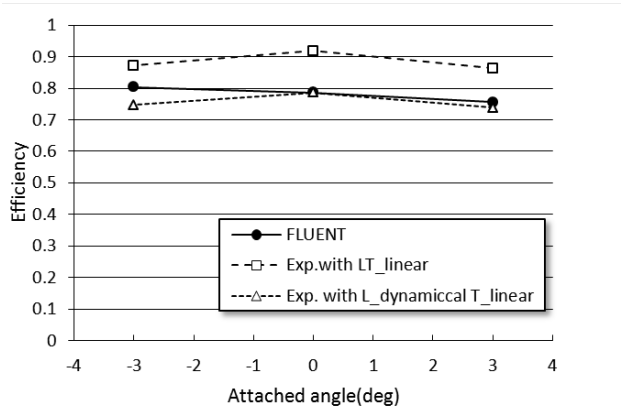

Fig. 10 Efficiency of Prop02 for 3 attached angles.

value by linear interpolation without estimation of stagnation point, it is clear that the method of the interpolation is appropriate.

4.2 Local thrust, torque, and efficiency of each blades

Figs. 11 - 16 show the amount of the partial thrust and torque along the span direction of each blade. In this figure, the blade

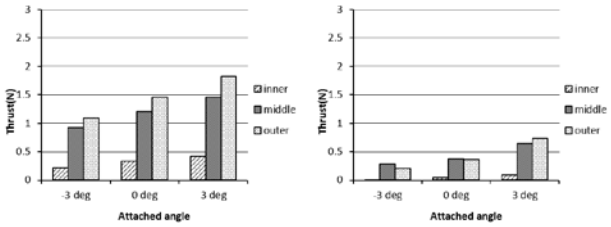

a) Camber Side b) Thrust Side

Fig. 11 Partial Thrust of Prop 00.

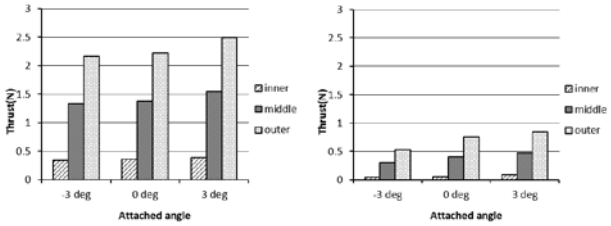

a) Camber Side b) Thrust Side

Fig. 12 Partial Thrust of Prop 01.

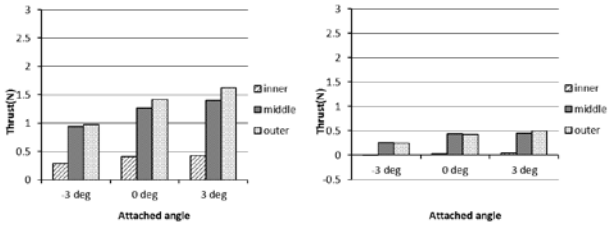

a) Camber Side b) Thrust Side

Fig. 13 Partial Thrust of Prop 02.

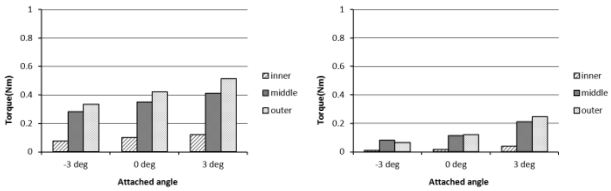

a) Camber Side b) Thrust Side

Fig. 14 Partial Torque of Prop 00.

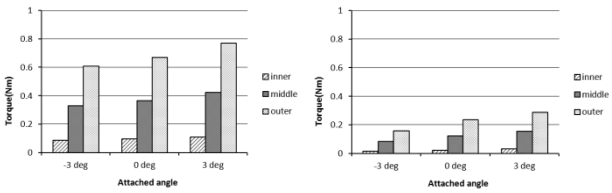

a) Camber Side b) Thrust Side

Fig. 15 Partial Torque of Prop 01.

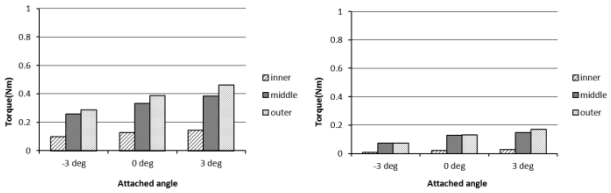

a) Camber Side b) Thrust Side

Fig. 16 Partial Torque of Prop 02.

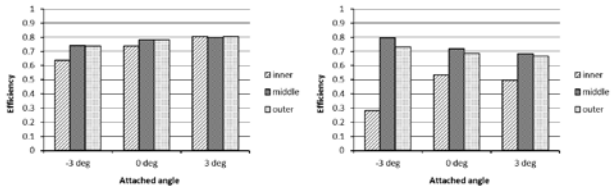

a) Camber Side b) Thrust Side

Fig. 17 Partial Efficiency of Prop 00.

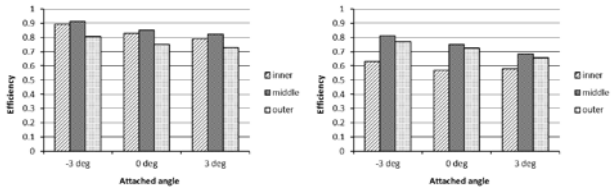

a) Camber Side b) Thrust Side

Fig. 18 Partial Efficiency of Prop 01.

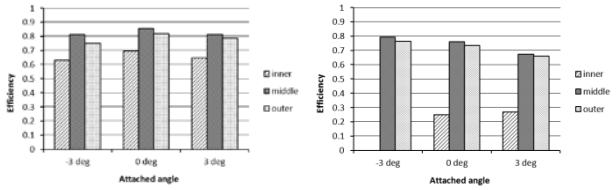

a) Camber Side b) Thrust Side

Fig. 19 Partial Efficiency of Prop 02.

is divided up 6 regions as “inner”, “middle”, and “outer” on the camber surface and thrust surface. The purpose is simplifying to compare the each characteristic among the different planar shape.

As shown in Figs. 11, 12, and 13, thrust generated at inner and middle region of each blade has almost no difference, but at the outer region, the thrust generated by prop01 is the largest because its area becomes wider as the span position is outer side. By contrast, the thrust couldn’t be generated at inner region of Prop02 in comparison with its chord length as shown in Fig. 13 a).

Thrust is generated mainly at the middle and outer region of the blade. On the Prop00 blade, rates of the thrust generated at middle and outer region for -3 degree, 0 degree, and 3 degree are 91.8%, 90.4%, and 90.3%, respectively. And, for the other blade, the average rates among their 3 attached cases are 92.0% (Prop01) and 89.6% (Prop02). This fact tells that an improvement of planar shape for outer side than middle region is effective. In light of the specification of the each planar shape of the blade, but, these rates appeared like a coy. In comparison with the thrust per unit area, Prop01 is less than Prop02, although the amount of thrust generated by Prop01 is larger than one of the Prop02.

As shown in Figs. 14, 15, and 16, there is a remarked difference of the torque generated at the outer region of Prop01 blade. And, the torque generated at the inner region of Prop02 blade is relatively larger than one at the same region of the other blades.

Most of torque is produced at the middle and outer region of blade. The rates in comparison with the whole surface of each blade are 89.9% (Prop00), 92.1% (Prop01), and 86.7% (Prop02).

Finally, the comparison of efficiency among the regions of each blade shows in Figs. 17, 18, and 19. On the camber surface of Prop00 blade, the efficiencies at three regions increase slightly as attached angle increases, and efficiencies of three regions similar at each attached angle as shown in Fig.17 a). This tendency probably is caused by the influence of the method of the optimum shape design. On the camber surface of Prop01, the efficiencies decrease as attached angle increases, and especially the value of outer region at every attached angle is worse in comparison with the other regions because of the spread shape on the tip side as shown in Fig. 18 a). By contrast with the difference of the change of efficiencies among the attach angle on the camber surface, the efficiency on the thrust surface decreases as attached angle increases out of relation of the difference in the planar shape of blade as shown in Figs. 17 b), 18 b), and 19 b). So, there is a tendency that efficiency evaluated by whole blade becomes worse owing to the characteristic of the thrust surface. But, this tendency of the decline is probably caused by the shape of the cross section, which is FX63-137 airfoil.

5 Conclusions

In order to compare the characteristic related with planar shape, wind tunnel testing and CFD simulation were performed for 3 types of blade. Even if there is a local area in where the pressure can’t be obtained, for example, near leading edge, trailing edge, tip and root of blade, the data on whole surface of blade can be

obtained by the application of appropriate interpolation.

The partial characteristic of 3 types of blade can represented some specifications that result from planar shape of blade. Prop00 blade, which has the optimum planar shape, has the almost constant efficiency along the span direction. Prop01 blade received the torque larger than other blade at the outer part, but not only generated the thrust. Eventually, the efficiency is the worst in comparison with the other blade. The characteristic of Prop02 is similar to the one of Prop00, and the efficiency of the middle part is rather higher than one of Prop00 blade. It can be said that trapezoid blade can obtain the high efficiency without the particular design. As mentioned above, differences in characteristic among blades could be obtained from partial evaluation of thrust, torque, and efficiency.

References

[1] Adkins, C. N.and Leibeck, R. H., Design of optimum propellers, AIAA Paper-83-0190, 1983.

[2] Betz, A. with appendix by Prandtl, L., Screw Propellers with Minimum Energy Loss, Gottingen Reports, 1919.

[3] Ichiro Tani, Low-speed flows involving bubble separations, Progress in Aeronautical Science, 5, Pergamon Press, pp.70-103, 1964.

Copyright Statement